



The guanine nucleotide exchange factor RapGEF2 is required for ERK-dependent immediate-early gene (Egr1) activation during fear memory formation

Sunny Zhihong Jiang¹ · Meishar Shahoha² · Hai-Ying Zhang¹ · William Brancaleone¹ · Abdel Elkahloun⁴ · Hugo A. Tejada³ · Uri Ashery² · Lee E. Eiden¹

Received: 24 April 2023 / Revised: 16 September 2023 / Accepted: 4 October 2023

This is a U.S. Government work and not under copyright protection in the US; foreign copyright protection may apply 2024

Abstract

The MAP kinase ERK is important for neuronal plasticity underlying associative learning, yet specific molecular pathways for neuronal ERK activation are undetermined. RapGEF2 is a neuron-specific cAMP sensor that mediates ERK activation. We investigated whether it is required for cAMP-dependent ERK activation leading to other downstream neuronal signaling events occurring during associative learning, and if RapGEF2-dependent signaling impairments affect learned behavior. *Camk2α-cre^{+/-}::RapGEF2^{fl/fl}* mice with depletion of RapGEF2 in hippocampus and amygdala exhibit impairments in context- and cue-dependent fear conditioning linked to corresponding impairment in *Egr1* induction in these two brain regions. *Camk2α-cre^{+/-}::RapGEF2^{fl/fl}* mice show decreased RapGEF2 expression in CA1 and dentate gyrus associated with abolition of pERK and *Egr1*, but not of c-Fos induction, following fear conditioning, impaired freezing to context after fear conditioning, and impaired cAMP-dependent long-term potentiation at perforant pathway and Schaffer collateral synapses in hippocampal slices *ex vivo*. RapGEF2 expression is largely eliminated in basolateral amygdala, also involved in fear memory, in *Camk2α-cre^{+/-}::RapGEF2^{fl/fl}* mice. Neither *Egr1* nor c-fos induction in BLA after fear conditioning, nor cue-dependent fear learning, are affected by ablation of RapGEF2 in BLA. However, *Egr1* induction (but not that of c-fos) in BLA is reduced after restraint stress-augmented fear conditioning, as is freezing to cue after restraint stress-augmented fear conditioning, in *Camk2α-cre^{+/-}::RapGEF2^{fl/fl}* mice. Cyclic AMP-dependent GEFs have been genetically associated as risk factors for schizophrenia, a disorder associated with cognitive deficits. Here we show a functional link between one of them, RapGEF2, and cognitive processes involved in associative learning in amygdala and hippocampus.

Keywords cAMP · MAP kinase · Immediate early gene · c-Fos · *egr1/zif268* · Fear learning

Sunny Zhihong Jiang and Meishar Shahoha have equal contribution to this report.

✉ Uri Ashery
uriashery@gmail.com

✉ Lee E. Eiden
eidenl@mail.nih.gov

¹ Section On Molecular Neuroscience, NIMH Intramural Research Program, 9000 Rockville Pike, Building 49, Room 5A38, Bethesda, MD 20892, USA

² School of Neurobiology, Biochemistry and Biophysics, George S. Wise Faculty of Life Sciences, and Sagol School of Neuroscience, Tel Aviv University, Sherman Building Rm 719, Ramat Aviv, 69978 Tel Aviv, Israel

³ Unit on Neuromodulation and Synaptic Integration, NIMH-IRP, Bethesda, MD, USA

⁴ Microarray Core, NHGRI-IRP, Bethesda, MD, USA

Introduction

The events associated with neuronal synaptic transmission are now relatively well understood [1], while the neurotransmission-associated molecular changes required to enable experience-based learning and memory remain to be fully explored and put into a coherent cellular model [2, 3]. Neurons contain ‘cognitive kinases’ that respond to the second messengers calcium and cyclic AMP to allow induction of immediate early genes (IEGs) and synaptic potentiation, two processes through which cellular plasticity, and the encoding of experience as learning and memory, occurs [4, 5]. Cyclic AMP, in particular, mediates neuronal changes linked to altered synaptic function [6] and subsequent behavior responses [2, 7]. Neurotransmitters such as catecholamines and serotonin cause cAMP elevation via ligand-activated

guanine nucleotide exchange factors (GPCRs) coupled to G_s . Cyclic AMP can also act as a *third* messenger in neurons, after calcium-dependent adenylyl cyclase activation triggered by neuronal depolarization [8].

Protein kinase A is the major protein kinase activated by cAMP [9–11], with CREB as its downstream effector for several forms of synaptic plasticity [2, 12]. The MAP kinase ERK also has a critical role in neuronal plasticity, but how it is activated by cAMP is unclear [13, 14]. Attempts to define the cAMP-initiated pathways leading to ERK and CREB signaling are illustrated in seminal reports on the role(s) of Rap and PKA in mediating ERK-dependent aspects of long-term potentiation (LTP) important for hippocampal-dependent memory tasks [15, 16]. Several other protein kinases [13, 17–21] have been linked to various types of LTP [22] considered to be intercellular mechanism(s) for encoding associative memory [23]. Forging the key molecular links between cAMP and ERK signaling, given the apparent centrality of both for associative learning in rodents underlying spatial memory and fear conditioning [24], is an important problem in neurobiology.

The discovery of two guanine nucleotide exchange factors (GEFs), Epac1 and Epac2, that respond to cAMP by activation of the small GTPase Rap, seemed to provide a PKA-independent pathway for activation of ERK via cAMP [25–27], but further analysis revealed that Epac does not activate ERK [28]. Subsequently, however, a neuron-specific GEF, RapGEF2, was identified as a cAMP effector that preferentially activates ERK in neuroendocrine cells [29, 30].

A signaling matrix in which cAMP activates cognitive kinases through parallel PKA-dependent and PKA-independent pathways is an attractive construct for better understanding the molecular events controlling neuronal plasticity. For example, dopamine signaling through the D1 G_s PCR activates both CREB and ERK phosphorylation in D1 dopamine neurons [31], and eliminating RapGEF2 from D1 medium spiny neurons of the nucleus accumbens curtails cocaine-induced locomotor sensitization and conditioned place preference [32], the latter known to require ERK signaling [33]. RapGEF2 is also implicated in development of neuronal maturation [34], and in Rap signaling involved in synaptic plasticity in hippocampal dendritic spines [35], although its function in cAMP-dependent memory and learning processes has never been addressed.

In this report, we explore the role of neuronal RapGEF2 in aversive associative memory formation during cue- and context-dependent fear conditioning (FC), by comparing IEG induction and ERK activation in hippocampus and amygdala, and subsequent freezing behavior, in wild-type and $Camk2\alpha$ -cre^{+/+}::RapGEF2^{fl/fl} mice. RapGEF2 expression is ablated in excitatory neurons of hippocampus and amygdala in these mice. The effects of RapGEF2 ablation in CA1 and dentate gyrus on long-term post-synaptic potentiation,

in both the Schaffer collateral and perforant pathways, were compared to effects of RapGEF2 ablation on IEG induction in both hippocampus and amygdala. Effects of RapGEF2 ablation on IEG induction in amygdala were examined in both cue and context-associated FC, and in FC augmented with restraint stress. The data obtained argue for consideration of RapGEF2 as a cAMP sensor required for neuronal signaling in hippocampus and amygdala that mediates the pairing of conditioned and unconditioned stimuli required for associative learning.

Results

Ablation of RapGEF2 protein expression in hippocampal CA1 and DG

A $Camk2\alpha$ -cre^{+/+}::RapGEF2^{fl/fl} mouse line [31] previously shown to exhibit RapGEF2 deletion in cortical and amygdalar excitatory neurons was employed [32]. RapGEF2 protein expression is also ablated in mouse hippocampus in an age-dependent manner. RapGEF2 immunostaining was reduced ~50% in hippocampal CA1, but not in DG or CA3, at postnatal age 5 weeks in $Camk2\alpha$ -cre^{+/+}::RapGEF2^{fl/fl} (cKO) mice (Fig. 1a, left panel) and largely eliminated in both CA1 and DG areas by age 10 weeks (Fig. 1a, right panel and b), with $11.83 \pm 4.28\%$ remaining in CA1 and $11.43 \pm 2.68\%$ remaining in DG of cKO hippocampus based on quantitative immunostaining. No reduction was observed in the CA3 region. Similar results were obtained by Western blot using protein lysates from subregions of the hippocampus (Fig. 1c, left panel). Only $18.13 \pm 3.75\%$ of RapGEF2 protein remained in CA1 and $21.03 \pm 5.63\%$ remained in DG in cKO hippocampus (Fig. 1c, right panel). $Camk2\alpha$ -cre^{+/+}::RapGEF2^{fl/fl} mice older than 10 weeks also showed RapGEF2 knock-down in basolateral amygdala but not central amygdala (Fig. 1d; $10.85 \pm 1.39\%$ of RapGEF2 protein remaining in BLA of cKO compared to WT mice).

Contextual fear memory consolidation is impaired following RapGEF2 protein ablation in hippocampus

Mice were subjected to serial behavioral tests to assess effects of RapGEF2 ablation on behaviors unrelated to learning and memory: home cage monitoring (Figure S1a), elevated zero maze (Figure S1b), open field (Figure S1c) and rotarod tests were performed (Figure S1d). $Camk2\alpha$ -cre^{+/+}::RapGEF2^{fl/fl} (cKO) did not show differences from RapGEF2^{fl/fl} control mice in locomotor activity, exploration, anxiety, or balance and motor coordination. The Patterned Barnes Maze (PBM) was used to examine hippocampus-dependent spatial learning and memory (Figure S1e ~ S1h and Figure S2a). cKO and flox controls showed similar

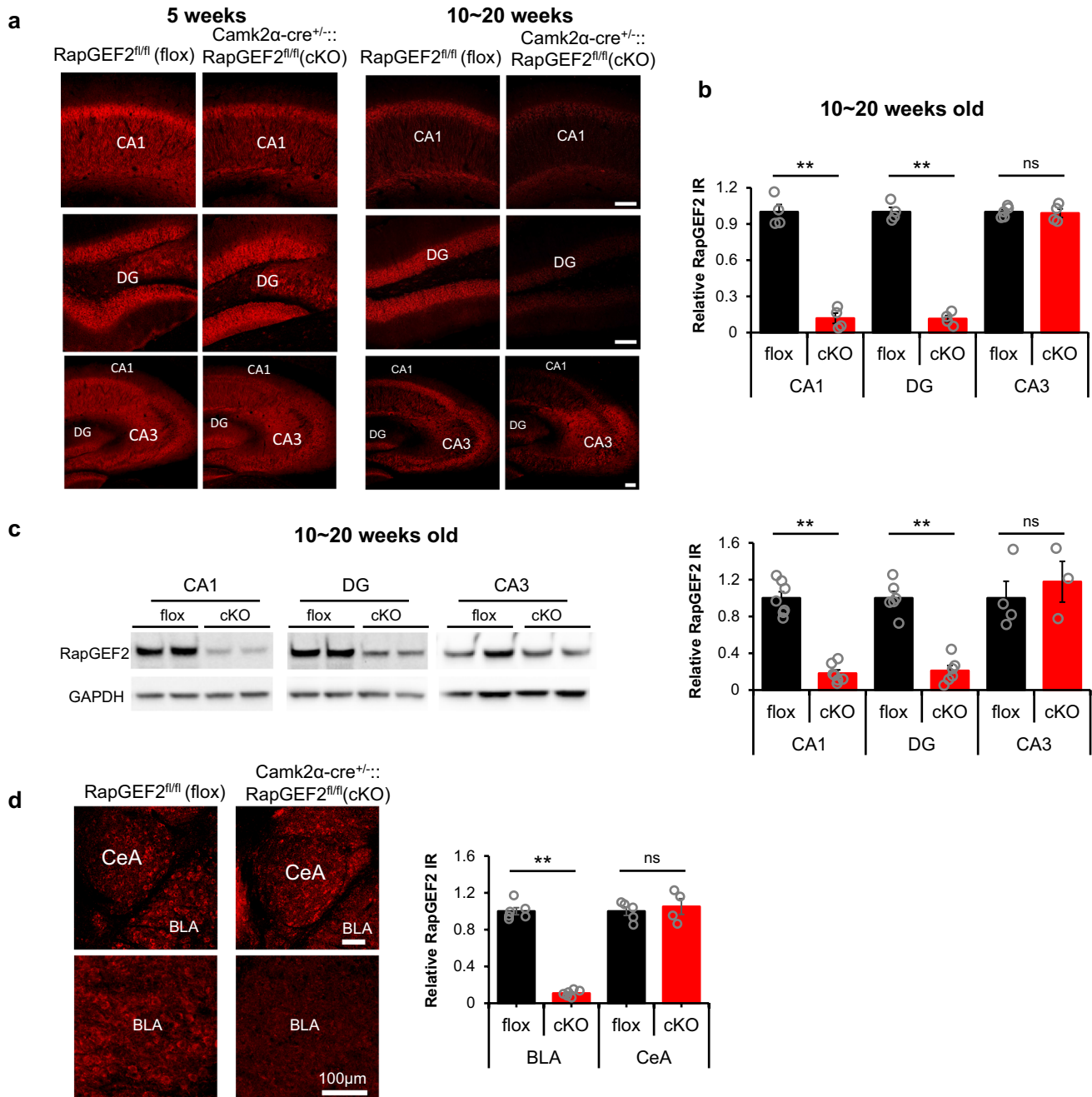
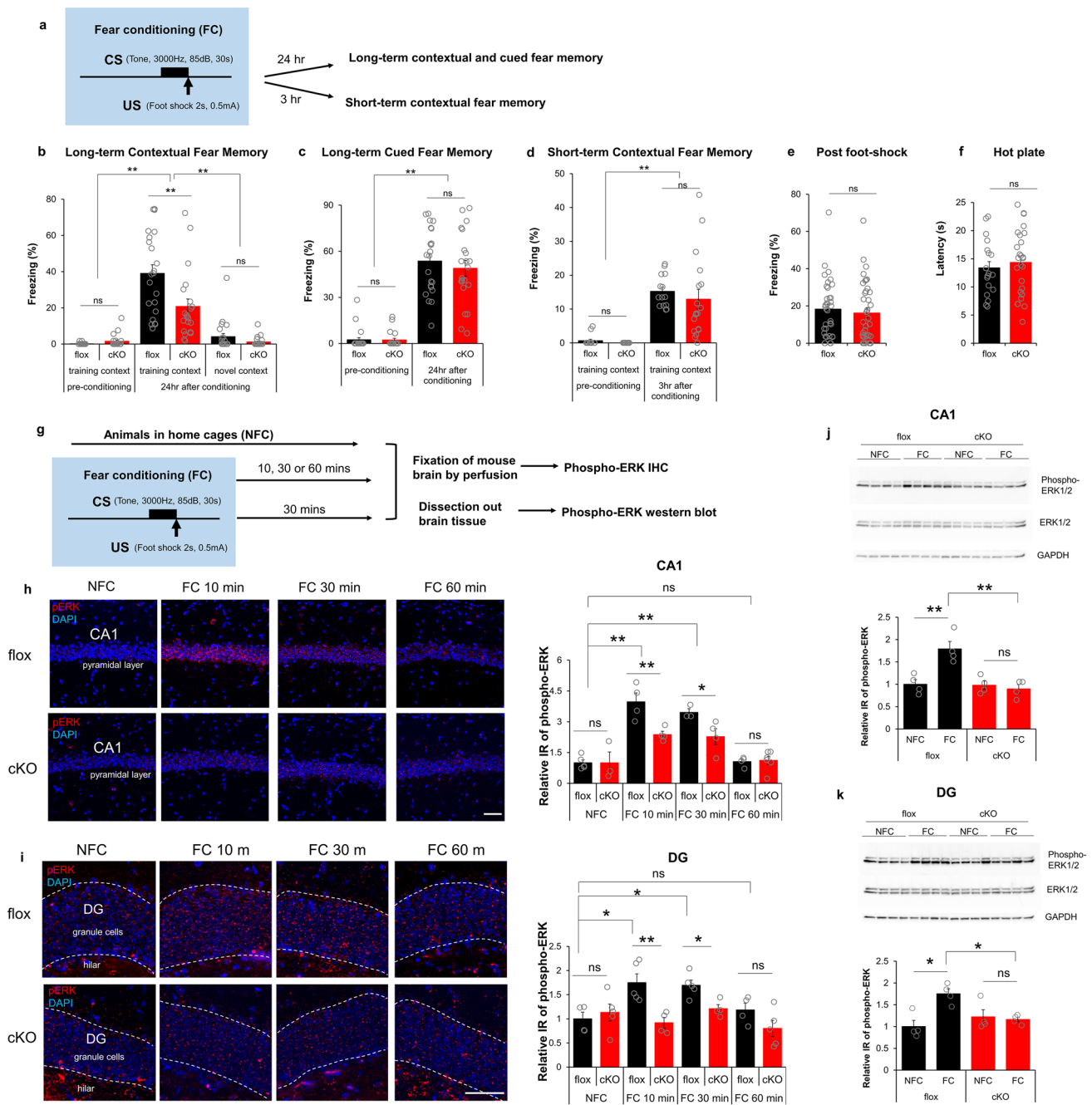


Fig. 1 Ablation of RapGEF2 protein expression in hippocampal CA1, DG and BLA. **a** Representative immunohistochemical images with RapGEF2 antibody (NNLE-2) for hippocampal subregions (CA1, DG and CA3) from floX and cKO mice at 5-weeks old (left panel) and 10~20 weeks old (right panel). Scale bar: 100 μm. **b** RapGEF2 immunoreactive (IR) signals in hippocampal CA1, DG and CA1 from cKO mice (10~20 weeks old) were quantified with NIH Image J and compared to RapGEF2 IR signals from floX mice. The result indicated a significant reduction in RapGEF2 levels in the CA1 and DG hippocampal subregions, but not in the CA3 subregion. N=4~5 for animal number in each group. Student's t-test for each region,

** $p < 0.001$. **c** Western blots using protein lysates from hippocampal subregions of floX and cKO mice showed similar results that RapGEF2 was downregulated in CA1 and DG. N=3~7 for animal number in each group, Student's t-test for each region, ** $p < 0.001$. **d** RapGEF2 immunoreactive (IR) signals in Amygdala from floX and cKO mice (10~20 weeks old) showed that RapGEF2 expression in BLA was significantly reduced in BLA, but not in CeA. Quantitative assessment of RapGEF2 levels in BLA of wild-type and Camk2α-cre^{+/+}::RapGEF2^{fl/fl} mice has been previously reported (see Fig. 4B in [32])



learning curves (Figure S1f) and similar time to locate the target hole in the probe trial (Figure S1f~S1h), indicating normal locomotor activity, exploration, balance and motor coordination, and spatial navigation and memory, in RapGEF2 cKO mice.

Contextual fear conditioning is hippocampus-dependent, while both contextual and cued fear conditioning require the BLA [36, 37]. To test for deficits in contextual and/or cued FC in RapGEF2-deficient mice, FC procedures were conducted with both contextual and auditory components, with mice learning to associate a tone (85 dB,

3 kHz, 30 s, co-terminated with foot shock) with an electric foot shock (0.5 mA, 2 s), within a specific training chamber (context) (Fig. 2a, S2b). Contextual fear memory was tested 24 h after fear conditioning by measuring freezing in training or novel chambers (Fig. 2b, S2b). Both floxed and cKO mice could distinguish between training and novel contexts. However, cKO mice showed significant reduction in freezing in the training context compared to controls. Although RapGEF2 is ablated in BLA in cKO mice [31, 32] (Fig. 1d), they had no deficits in cued fear

Fig. 2 Camk2 α -cre^{+/+}::RapGEF2^{fl/fl} (cKO) mice show deficit in consolidation of contextual fear memory. **a–f** Consolidation of contextual fear memory was impaired in Camk2 α -cre^{+/+}::RapGEF2^{fl/fl} mice. The scheme of a fear conditioning test used for cKO and floxed control mice (**a**). cKO mice showed impaired contextual memory to the training context, not novel context, 24 h later compared to controls (**b**). However, both floxed and cKO mice showed normal levels of freezing during the tone presentation in a non-training context when memory was retrieved 24 h after conditioning (**c**). Two-way ANOVA following by post hoc Bonferroni t-test, ***p*<0.001. N=22 for animal number of floxed mice, N=21 for animal number of cKO mice. Contextual freezing 3 h after the conditioning was similar between cKO and floxed mice, suggesting acquisition and retrieval of memory was not affected in cKO mice (**d**). Two-way ANOVA following by post hoc Bonferroni t-test, ***p*<0.001. N=14 for animal number of floxed mice, N=18 for animal number of cKO mice. Floxed and cKO mice showed similar freezing level immediately after foot-shock during fear conditioning (**e**, N=36 for floxed mouse number, 39 for cKO mouse number) and similar latency in a hot plate test (**f**, N=19~26 for animal number in each group), suggesting no differences in pain sensitivity between two groups. **g–k** ERK activation in hippocampus during fear conditioning is RapGEF2-dependent. The experimental procedure to examine ERK activation after fear conditioning (**g**). Representative images of phospho-ERK staining (in red) in hippocampal CA1 pyramidal cell layer (**h**, panels on the left) or hippocampal DG granule cell layer (**i**, panels on the left) of floxed and cKO mice 10 min (FC10 min) or 30 min (FC 30 min) or 60 min (FC 60 min) after fear conditioning or without fear conditioning (NFC). Scale bar: 50 μ m. Immunoreactive (IR) signals of phospho-ERK in the CA1 or DG of floxed and cKO mice at different time points after fear conditioning were quantified by NIH Image J using the mean gray values of integrated density after being converted to gray scale; then compared to average value from mice in the home cage (NFC) to obtain “Relative IR of phospho-ERK” (**h** and **i**, panels on the right). N=3~5 for animal number in each group. Two-way ANOVA following by post hoc Bonferroni t-test, **p*<0.05; ***p*<0.001. Phospho-ERK activation in hippocampal CA1 and DG were also quantified with western blot (**j** and **k**). Hippocampal CA1 or DG were dissected out from floxed or cKO mice 30 min post fear conditioning (FC) or without fear conditioning (NFC). Protein lysates were subjected to western blots with phospho-ERK, pan-ERK and GAPDH antibodies. N=4 for animal number in each group. Protein bands from western blots were quantified using imageJ and GAPDH protein served as internal controls to normalize the loading. Phospho-ERK IR from different groups was compared to average value from floxed mice in the home cage (NFC), to obtain “Relative IR of phospho-ERK”. Two-way ANOVA following by post hoc Bonferroni t-test, **p*<0.05; ***p*<0.001

memory when tested 24 h after fear conditioning (Fig. 2c). Attenuation of contextual freezing 24 h after FC in cKO mice was not due to impaired acquisition or retrieval of memory, as contextual freezing 3 h after conditioning was unaffected (Fig. 2d). Floxed and cKO mice showed similar freezing levels immediately after foot-shock during FC (Fig. 2e) and similar latency in a hot plate test (Fig. 2f), suggesting no differences in pain sensitivity between the two groups. In summary, hippocampus-dependent contextual fear memory consolidation was selectively impaired in Camk2 α -cre^{+/+}::RapGEF2^{fl/fl} mice. This effect is selective for fear memory, as performance in the Barnes maze, another hippocampus-dependent task, was unaffected.

ERK activation in hippocampus during fear conditioning (FC) is RapGEF2-dependent

RapGEF2 is a cAMP sensor/effector linking Gs-coupled GPCR signaling to ERK in adult neurons and neuroendocrine cells [31, 38–40]. It has been previously demonstrated that phospho-ERK induction in hippocampus occurs during shock associated with context, but not in animals exposed only to the context, nor in animals shocked immediately without contextual paired experience [21, 41]. To investigate whether RapGEF2 contributed to contextual fear memory consolidation via ERK signaling, hippocampal CA1 and DG sections were collected from floxed control and cKO mice at 10, 30, or 60 min after FC, and immunostained with phospho-ERK antibody (Fig. 2g). Sections from animals kept in the home cage (without fear conditioning, NFC) were used as controls. Floxed mice showed a significant increase in phospho-ERK in CA1 at 10 min or 30 min following FC, returning to home cage control levels at 60 min. cKO mice showed attenuation of phospho-ERK activation 10 min or 30 min after FC (Fig. 2h). Similarly, cKO mice showed attenuation of phospho-ERK activation in DG at 10 or 30 min following FC compared to floxed control mice (Fig. 2i). Western blots with tissues collected from hippocampal CA1 or DG 30 min after fear conditioning also demonstrated that ERK activation in hippocampal CA1 and DG during FC is RapGEF2-dependent (Fig. 2j and k).

Basal synaptic properties and short-term plasticity are intact in Camk2 α -cre^{+/+}::RapGEF2^{fl/fl} mice in the Schaffer collateral and the medial perforant pathways

RapGEF2-dependent signaling may modify hippocampal synaptic function essential for contextual fear conditioning. To determine this, we utilized ex vivo slice electrophysiology, focusing on two primary hippocampal synapses: the CA3-CA1 Schaffer collateral pathway (SC) synapse, and the medial perforant pathway (MPP) entorhinal cortex to DG synapse. Both exhibit robust synaptic plasticity and are implicated in fear-related memory generation in contextual FC procedures. We first generated input–output (I/O) curves measuring the relationship between the amplitude of the fiber-volley trace and the amplitude of the resulting electrically-evoked fEPSP at SC and MPP synapses. Neither the EPSP amplitudes nor the fiber-volley were significantly different from controls for either SC (Fig. 3a) or MPP synapses (Fig. 3b), indicating similar baseline synaptic efficacies in cKO and floxed control mice. Changes in short-term plasticity (STP) are indicative of presynaptic properties such as neurotransmitter release probability (P_r). We tested effects of RapGEF2 deletion on P_r and short-term plasticity (STP) in the SC

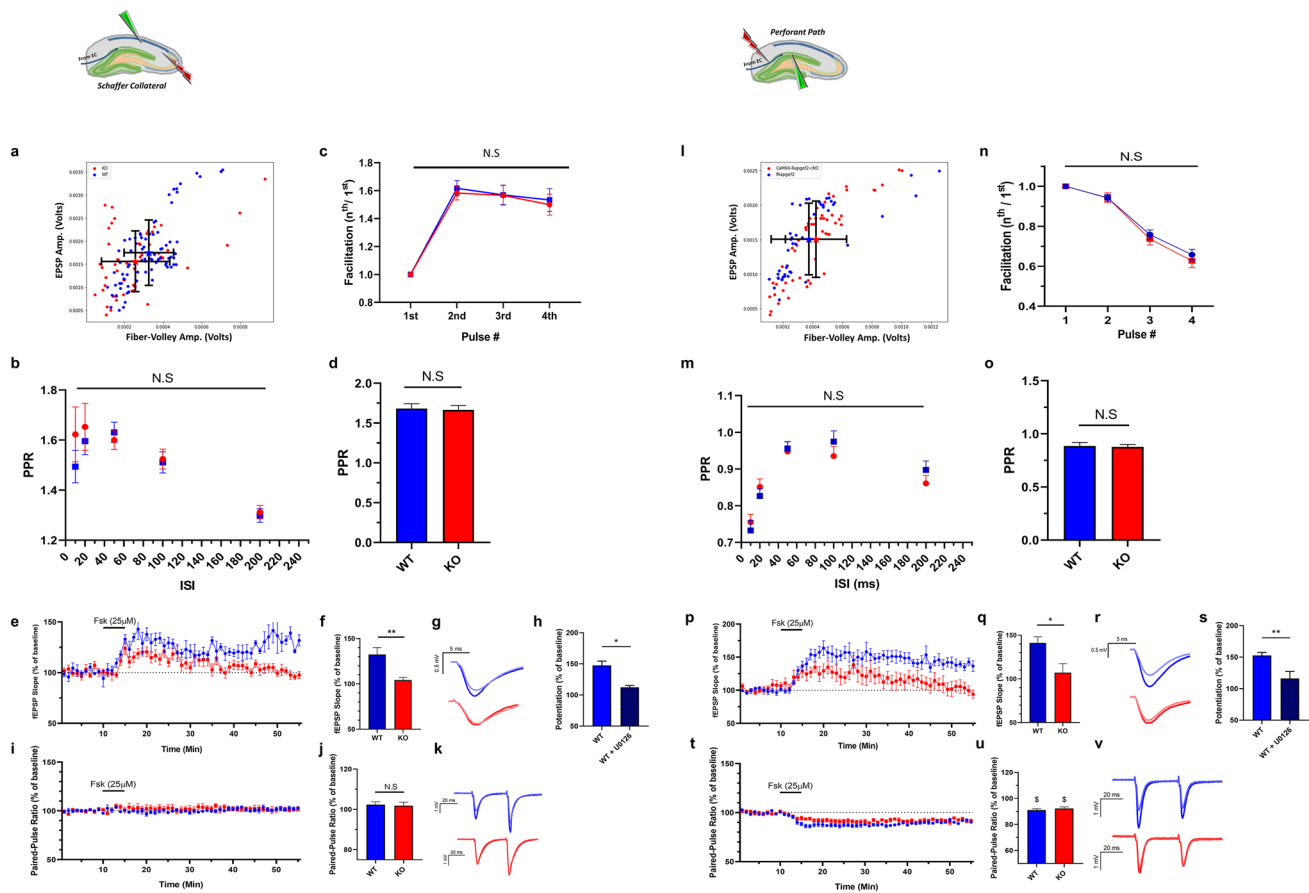


Fig. 3 Comparison of short-term plasticity properties between *Camk2α-cre^{+/::}RapGEF2^{fl/fl}* and WT mice. Results are shown symmetrically for the SC (**a–k**) and MPP (**l–v**) pathways. **a** and **l** Input/Output (I/O) curves obtained from *RapGEF2^{fl/fl}* (blue trace) and *Camk2α-cre^{+/::}RapGEF2^{fl/fl}* (red trace) mice. $N=8$ slices, 4 mice per group. $p>0.05$ for SC and MPP. **b** and **m** Results from a comparison of PPR values at different inter-spike intervals (ISIs). $N=7–11$ slices, 4–6 mice, per group. Two-way repeated-measures ANOVA, $p>0.05$. **c** and **n** Facilitation pattern that results from a burst of 4-stimulations given at 25 Hz. $N=7–11$ slices, 4–6 mice, per group. Two-way ANOVA, $p>0.05$. **d** and **o** A summary of the baseline PPR values obtained during subsequent experiments presented in **e** and **p**. $ISI=40$ ms. $N=9–14$ slices, 5–7 mice, per group. Two-way ANOVA, $p>0.05$. **e** and **p** fEPSP slopes measurements before and after Fsk application. Results are shown for the two experimental groups; *Camk2α-cre^{+/::}RapGEF2^{fl/fl}* (red) and their WT littermates (blue). $N=4–10$ slices, 3–5 mice per group. Two-way repeated-measures ANOVA, $p=0.0174$ (SC) and $p=0.0371$ (MPP). **f** and **q** Summary

and MPP synapses. There were no genotype-dependent differences in paired-pulse ratios (PPR) obtained at different inter-spike intervals (ISIs used; 10, 20, 50, 100 and 200 ms), suggesting similar basal P_r in cKO and floxed controls (Fig. 3b and m). We also tested the facilitation pattern associated with a burst of four stimuli given with an ISI of 40 ms. Significant facilitation or depression are seen following such stimulation in the SC and MPP, respectively. Consistent with the aforementioned results,

results of fEPSP slopes show a significant impairment of Fsk-induced potentiation in slices obtained from *Camk2α-cre^{+/::}RapGEF2^{fl/fl}* animals, unpaired student's t-test, $p=0.001$ (SC), $p<0.01$ (MPP). **g** and **r** Representative traces of fEPSPs before (faint color) and 40 min after (bold color) Fsk administration for WT (blue) and *Camk2α-cre^{+/::}RapGEF2^{fl/fl}* (red) conditions. **h** and **s** Results from comparing WT (floxed) slices that were applied with Fsk only, and slices that had a prior preincubation with U0126 (20 μ M), and then applied with Fsk, show a significant decrease in potentiation. Unpaired student's t-test, $p=0.01236$ (SC), $p=0.0055$ (MPP). **i** and **t** PPR measurements show no change in PPR values following Fsk administration in the SC pathway. On the other hand, similar measurements in the MPP show slight decrease in PPR values to a similar degree across genotypes. Two-way repeated-measures ANOVA, $p>0.05$). **j** and **u** PPR mean values 40 min after Fsk application for the two experimental groups. **k** and **v** Representative traces of paired-pulse recordings before (faint color) and 40 min after (bold color) Fsk administration for WT (blue) and *Camk2α-cre^{+/::}RapGEF2^{fl/fl}* (red) conditions

cKO and floxed controls showed a similar burst facilitation/depression pattern (Fig. 3c and n). Finally, we compared PPR values measured during the baseline phase of the above experiments and found no significant differences between cKO and floxed control mice (Fig. 3d and o). Thus, cKO and floxed control mouse hippocampus appear identical in their basal synaptic and short-term plasticity properties.

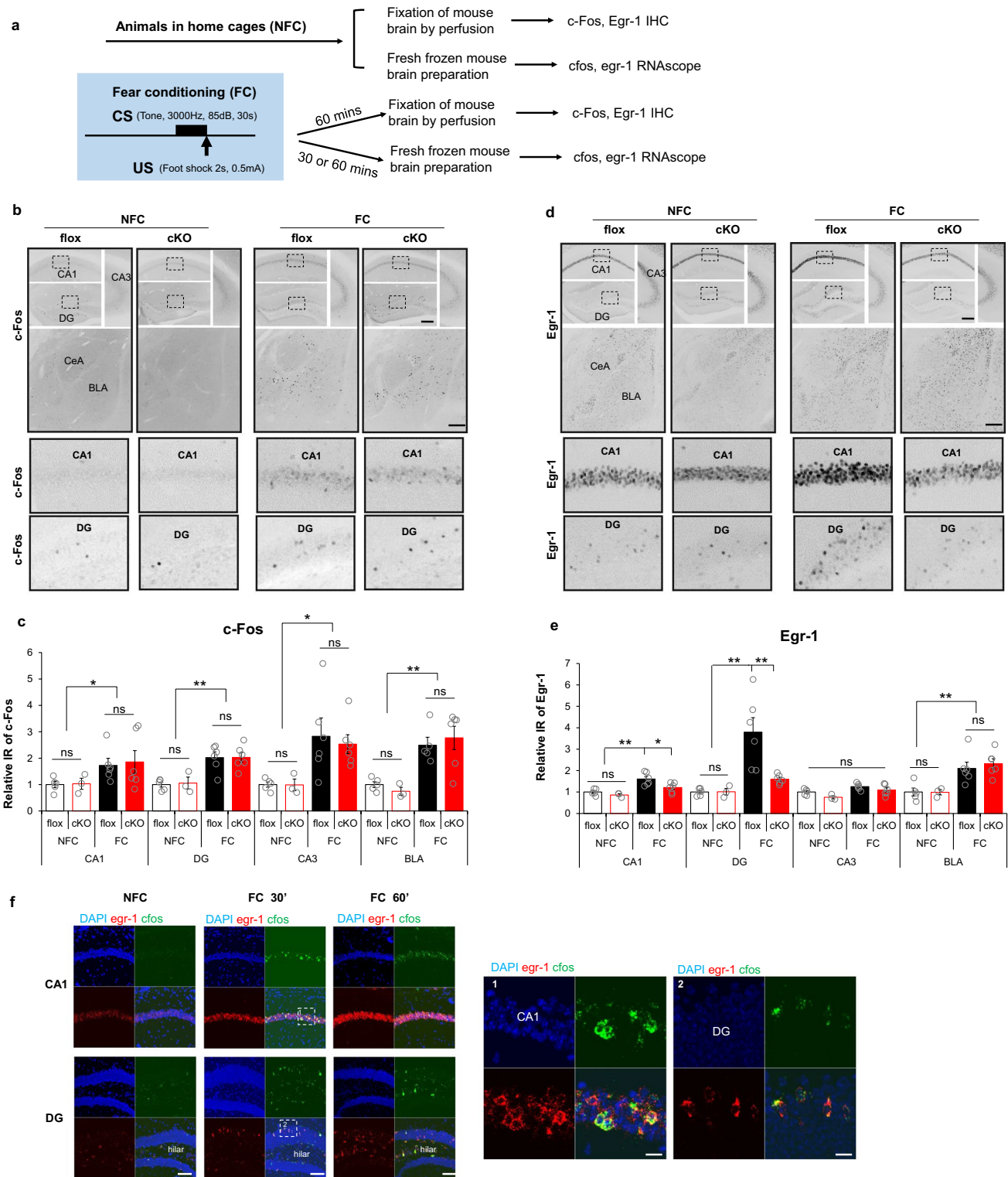
Camk2 α -cre^{+/-}::RapGEF2^{fl/fl} mice have impaired Fsk-induced SC-LTP and Fsk-induced MPP-LTP

Since RapGEF2 is a cAMP sensor, we tested RapGEF2 involvement in cAMP-dependent synaptic potentiation in SC synapses, comparing hippocampal slices obtained from Camk2 α -cre^{+/-}::RapGEF2^{fl/fl} mice and their floxed littermates for their ability to undergo Fsk-induced SC-LTP. After establishing a stable baseline of fEPSPs, Fsk was perfused into the recording chamber for five minutes, washed out using aCSF, and a subsequent 45 min of recording used to assess the effects of Fsk. Measurements of SC fEPSPs before and after Fsk application yielded a significant increase in fEPSP slopes following Fsk application in control slices, but not in cKO slices (Fig. 3e–g), implying that RapGEF2 is necessary for Fsk-induced potentiation at the SC-CA1 synapse. Furthermore, U0126 application abrogated Fsk-induced potentiation in control slices, consistent with a shared molecular pathway RapGEF2 → MEK → ERK in Fsk LTP (Fig. 3h). This form of LTP was not accompanied by any change in PPR, suggesting that RapGEF2-dependent Fsk-LTP is expressed postsynaptically at the SC-CA1 synapse (Fig. 3i–k).

The entorhinal cortex to granule cell (EC-DG synapse) pathway through the medial perforant path (MPP) also exhibits postsynaptic LTP; is implicated in various cognitive behavioral tasks; and shows post-synaptic (DG) RapGEF2 reduction in Camk2 α -cre^{+/-}::RapGEF2^{fl/fl} mice. Acute hippocampal slices obtained from either floxed control (RapGEF2^{fl/fl}) or cKO (Camk2 α -cre^{+/-}::RapGEF2^{fl/fl}) littermates were used for extracellular field recordings from the MPP. While slices from floxed controls showed 41.2 ± 6.94% increase in fEPSPs slopes compared to their baseline levels, which lasted for over 45 min (Fig. 3p–r), slices prepared from Camk2 α -cre^{+/-}::RapGEF2^{fl/fl} mouse brains showed an initial increase in synaptic efficacy, which gradually decreased to significantly lower levels relative to floxed control mice (107.1 ± 10.38) after around 40 min (Fig. 3p–r). As at the SC synapse, floxed control hippocampal slices exposed to U0126 during the entire recording showed reduction of Fsk-induced potentiation at the MPP synapse to levels seen in cKO mouse slices (Fig. 3s). In addition, we monitored changes in PPR by delivering a paired-pulse stimulation (ISI of 40 ms) via the stimulating electrode during these recordings. Application of Fsk was associated with a 10% decrease in the PPR in both floxed control and cKO mouse slices. These changes are consistent with a small increase in presynaptic release probability elicited by Fsk as cKO slices showed similar PPR levels at the MPP synapse following Fsk application (Fig. 3t–v). Our results indicate a post-synaptic role for RapGEF2 in cAMP-dependent LTP at both the SC and MPP synapses.

Differential dependency on RapGEF2 in fear conditioning-induced immediate early gene activation

Immediate-early genes (IEGs), such as *fos* and *egr1*, have been widely used as molecular markers for neuronal activation in cell culture [42, 43] and in vivo ([44], and [32] and references therein), especially in the context of genetic manipulation of hippocampal function required for memory formation [45–48]. Neuronal ensembles encoding fear memory may simultaneously express various IEGs. However the extent to which IEG-positive ensembles overlap with each other, and whether they are regulated separately in the same neurons, remains unclear. Quantification of IEG expression in floxed control and cKO hippocampus and amygdala was carried out 1 h after fear conditioning (Fig. 4a). Fos was induced after fear conditioning (Fig. 4b and c) throughout CA1, DG and CA3 in the hippocampus, and in BLA. RapGEF2 ablation had no effect on Fos expression (Fig. 4b and c). Egr-1 expression was also induced by fear conditioning in hippocampal CA1 and DG, but in contrast to *fos*, was RapGEF2-dependent (Fig. 4d and e). No genotype-specific IEG effects were observed in CA3. No genotype effect was observed for Egr-1 expression in BLA (Fig. 4d and e). We were therefore able to confirm the involvement of hippocampus, but not the BLA, in mediating the RapGEF2-dependent effects on contextual fear conditioning (but not cue fear conditioning), documented here. RapGEF2-dependent Egr-1 induction, but not c-Fos induction, after fear conditioning suggests that parcellated signaling pathways are involved in IEG induction. Taken together with the data presented in the previous section, these results strengthen the link between the involvement of RapGEF2 in Fsk-induced synaptic potentiation, and fear memory. Further characterization of fear conditioning induction of IEG mRNAs, by RNAscope with *egr1* and *fos* specific probes, indicated significant upregulation of *fos* mRNA in hippocampal CA1 and DG within 30 min following fear conditioning (Fig. 4f). *fos*-positive neurons in CA1 or DG are exclusively *egr1* positive. 68% ± 11% of *egr1*-positive neurons were *fos*-positive in CA1, and 88% ± 7.7% of *egr1*-positive neurons were *fos*-positive in DG (Fig. 4f). Thus, up-regulation of *fos* and *egr1* largely occurs in the same neuronal population(s) during fear conditioning. Furthermore, single-cell genomic analysis of wild-type mice (Figure S3) revealed that *fos* and *egr1* activation after fear conditioning occurs almost exclusively in Camk2 α positive neurons, i.e. the same population of neurons in which RapGEF2 is deleted in Camk2 α -cre^{+/-}::RapGEF2^{fl/fl} (cKO) mice. These observations support our working hypothesis that IEG up-regulation during fear conditioning is parcellated through separate cAMP-dependent signaling pathways, and that one



of them (*Egr1*) is RapGEF2 → ERK-dependent, and consequential for associative learning.

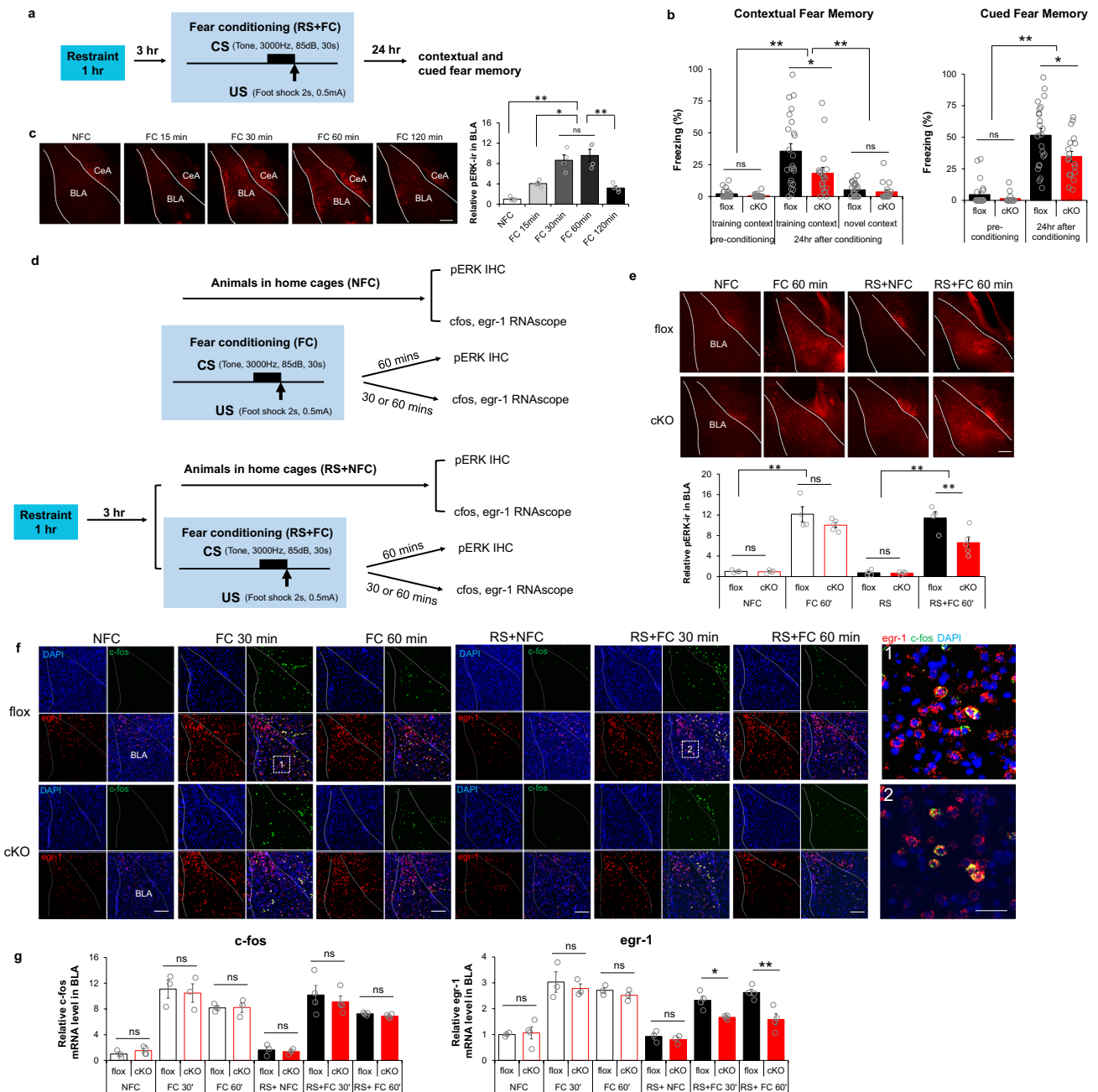
RapGEF2 expression is ablated not only in CA1 and dentate gyrus of hippocampus, but also in basolateral amygdala (BLA) and mPFC in *Camk2α-cre^{+/+}::RapGEF2^{fl/fl}* (cKO)

mice. However, there were no amygdala-associated impairments in cue-dependent fear memory or FC (Fig. 2) or in FC-associated IEG activation in *Camk2α-cre^{+/+}::RapGEF2^{fl/fl}* (cKO) mice (Fig. 4), compared to their RapGEF2-intact matched controls. Similarly, prominent induction of *fos* and

Fig. 4 Differential dependency of RapGEF2 in fear conditioning-induced immediate early genes activation in hippocampal CA1 and DG. **a** Experimental procedure to examine IEGs activation after fear conditioning. **b** Representative images of cFos immunostaining in hippocampal CA1, DG and CA3 and basolateral amygdala of flox and cKO mice that were sacrificed 1 h after fear conditioning (FC) or stayed in the home cage (NFC). Scale bar: 200 μm . Lower panels are images with higher magnification of the boxed areas in the upper panels. **c** Quantification of cFos immunoreactivity in hippocampal subregions and basolateral amygdala of flox and cKO mice indicated that fear-conditioning induced cFos increase in all these regions. Immunoreactive (IR) signals for c-Fos from different brain areas as indicated were quantified by NIH Image J using the mean gray values of integrated density after being converted to gray scale. C-Fos IR from different groups was normalized to average value from flox mice in the home cage (NFC), to obtain “Relative IR of c-Fos”. No significant difference was observed between flox and cKO mice. $N=3\sim 6$ for animal number in each group. Two-way ANOVA followed by post hoc Bonferroni t-test, $*p<0.05$, $**p<0.001$. **d** Representative images of Egr-1 immunostaining in hippocampal CA1, DG and CA3 and basolateral amygdala of flox and cKO mice after fear conditioning. Scale bar: 200 μm . Lower panels are images with higher magnification of the boxed areas in the upper panels. **e** Quantification of Egr-1 immunoreactivity indicated that the fear-conditioning induced Egr-1 increase in CA1 and DG is RapGEF2-dependent. Immunoreactive (IR) signals for Egr-1 from different brain areas as indicated were quantified by NIH Image J using the mean gray values of integrated density after being converted to gray scale. Egr-1 IR from different groups was normalized to the average value for flox mice in the home cage (NFC), to obtain “Relative IR of Egr-1”. cKO mice with RapGEF2 ablation in CA1 and DG showed attenuated Egr-1 increase in CA1 and DG 1 h after fear conditioning, compared to flox mice. $N=3\sim 6$ for animal number in each group. Two-way ANOVA followed by post hoc Bonferroni t-test, $*p<0.05$, $**p<0.001$. **f** RNAscope with *egr-1* (in red) and *c-fos* (in green) probes indicated that upregulation of *c-fos* mRNA in hippocampal CA1 and DG following fear conditioning occurred exclusively in the neurons with upregulation of *egr-1* mRNA. Quantification of *c-fos* and *egr-1* mRNA in hippocampal CA1 and DG 30 min after fear conditioning, $67.77\% \pm 10.92\%$ of *egr-1* positive neurons are *c-fos* positive in CA1; $87.89\% \pm 7.67\%$ of *egr-1* positive neurons are *c-fos* positive in DG. $N=3$ for animal number in each group. Scale bar: 100 μm (left panels), 20 μm (right panels)

egr1 in mPFC associated with FC was unaffected by cortical RapGEF2 deletion (i.e. in *Camk2 α -cre^{+/+}::RapGEF2^{fl/fl}* (cKO) compared to flox (control) mice), suggesting that this signaling pathway is not involved in cortical contributions to FC despite the presence of RapGEF2 in cortical in addition to hippocampal and amygdalar excitatory neurons (Supplementary Figure S4a,b). Likewise, we used potential RapGEF2 dependence of IEG profile to test whether RapGEF2 signaling is required for memory recall, rather than formation/consolidation. We examined *fos* and *egr1* levels in hippocampus 24 h after FC, at the time of presentation of the learned context for freezing (fear memory). We found no induction of Egr-1, and a robust induction of c-Fos, in hippocampus during memory recall; and found no differences between Egr-1 levels, or c-Fos induction, in *Camk2 α -cre^{+/+}::RapGEF2^{fl/fl}* (cKO) compared to flox (control) mice) at this time (Figure S4c,d).

Fear conditioning can be markedly modulated by stress, an effect associated with amygdalar circuitry [49], amygdalar activation of ERK [50, 51], and potentially involving cAMP-dependent signaling [52]. Accordingly, we introduced an acute stress component into our fear conditioning behavioral task. Animals received one hour acute restraint three hours before fear conditioning. Contextual fear memory was tested 24 h later by exposing mice to the training chamber or a novel chamber (Fig. 5a). Both floxed and cKO mice could distinguish between training and novel contexts. cKO mice showed reduced freezing compared to floxed controls when exposed to training context (Fig. 5b), similarly to their impaired performance in context-related fear memory in the absence of restraint stress (Fig. 2). However, when tested for cue association with shock following fear conditioning preceded by restraint stress, *Camk2 α -cre^{+/+}::RapGEF2^{fl/fl}* (cKO) mice showed significantly less freezing than their floxed control counterparts during tone presentation (Fig. 5b), suggesting that acute restraint stress prior to fear conditioning recruits a RapGEF2-dependent amygdalar circuit for cued-fear memory. These results offered the possibility to test whether ERK-dependent versus non-ERK-dependent IEG expression is also parcellated in cue-dependent FC in the amygdala, as for context-dependent FC and IEG expression in hippocampus. In BLA, phospho-ERK immunoreactivity increased most prominently at 30–60 min after FC (Fig. 5c). Brains were collected from *Camk2 α -cre^{+/+}::RapGEF2^{fl/fl}* (cKO) mice and their corresponding controls *RapGEF2^{fl/fl}* (flox) 30 or 60 min after FC, and in both restraint stressed and non-restraint stressed mice. Phospho-ERK levels in BLA were measured by IHC, and *fos* and *egr1* mRNAs were detected and visualized by RNAscope (Fig. 5d). ERK activation in the BLA was induced equivalently in floxed and cKO mice after FC alone. However, ERK activation in the BLA that occurred when acute restraint stress was applied prior to FC was significantly blunted in cKO compared to floxed mice (Fig. 5e). *Fos* mRNA expression in BLA was upregulated in both fear conditioning paradigms (Fig. 5f and g). *Fos* mRNA levels 30 min after fear conditioning (FC30) were higher than *fos* mRNA levels at 60 min (FC60). In contrast, *Egr1* mRNA induction induced by FC with prior restraint stress showed significant RapGEF2 dependency (Fig. 5f and g). Thus, no difference between cKO and floxed controls was detected in *egr1* mRNA expression when the 1 h restraint was not applied prior to FC, but restraint stress recruited a dependency on RapGEF2 for *egr1* mRNA induction in BLA (Fig. 5g). We also observed that upregulation of *fos* mRNA in BLA following fear conditioning occurred only in neurons in which *egr1* mRNA was also up-regulated (Fig. 5f).



Discussion

An extensive literature supports a requirement for ERK in contextual conditioned fear learning mediated by the hippocampal tri-synaptic pathway [12, 21, 24, 41, 53–55]. RapGEF2 signaling supports context-associated fear conditioning, based on RapGEF2 dependence of learning-associated ERK activation and Egr1 induction, cAMP-dependent synaptic potentiation, and fear conditioning itself. Cue-associated fear conditioning augmented by stress (restraint), where a requirement for ERK is also documented [49–51], is also associated with RapGEF2-dependent ERK

activation and Egr-1 induction in the amygdala, and is itself also impaired in RapGEF2 cKO mice.

Synaptic potentiation has long been invoked as a potential mechanism underlying associative learning [56, 57]. Its cellular and molecular properties have been studied extensively both in vivo and ex vivo [56]. Long term synaptic potentiation (LTP) may be elicited by elevation of cAMP [2, 15, 18, 58, 59], or by tetanic electrical stimulation of neuronal inputs involving recruitment of glutamate receptors to the post-synapse without an explicit cAMP requirement [22, 60]. Here we show that the biochemical hallmarks of cAMP-dependent LTP are consistent with a role in the creation

Fig. 5 Differential dependency of RapGEF2 in immediate early gene activation in basolateral amygdala after fear conditioning with prior restraint stress. **a** and **b** Both contextual and cued fear memory was impaired in *Camk2 α -cre^{+/+}::RapGEF2^{fl/fl}* mice (cKO) when 1 h restraint stress was applied 3 h prior to fear conditioning. Scheme of fear conditioning test employed is shown (**a**). cKO mice showed impaired contextual memory to the training context, not to a novel context, 24 h after conditioning, compared to controls (**b**, left panel). cKO mice showed attenuation in freezing during the tone presentation in a non-training context when memory was retrieved 24 h after conditioning (**b**, right panel). Two-way ANOVA followed by post hoc Bonferroni t-test, ****** $p < 0.001$, ***** $p < 0.05$. $N = 23$ flox mice, $N = 18$ cKO mice. **c** ERK activation in BLA after fear conditioning. pERK immunoreactivity (ir) in amygdala of RapGEF2^{fl/fl} mice sacrificed at 15, 30, 60 min or 120 min after fear conditioning (FC15 min, FC 30 min, FC 60 min or FC 120 min) or from mice that stayed in home cage (NFC). Phospho-ERK IR in the BLA at different time points after fear conditioning was quantified using ImageJ, showing most prominent activation in BLA occurring 30–60 min after fear conditioning. $N = 4$ for animal number in each group. One-way ANOVA followed by post hoc Bonferroni t-test, ****** $p < 0.001$, ***** $p < 0.05$. Scale bar: 200 μm . **d** Experimental procedure to examine phospho-ERK and IEGs activation in BLA after fear conditioning without or with restraint stress. **e** ERK activation in the BLA of cKO mice 1 h after fear conditioning was not significantly different from that of flox mice. However, phospho-ERK IR level in the BLA was attenuated in cKO mice when acute restraint stress was applied prior to fear conditioning. $N = 4\text{--}5$ for animal number in each group. Two-way ANOVA followed by post hoc Bonferroni t-test, ****** $p < 0.001$. Scale bar: 200 μm . **f** Representative RNAscope images of *c-fos* (green) and *egr-1* (red) in basolateral amygdala of flox and cKO mice that were sacrificed 30 min or 1 h after fear conditioning with or without restraint stress. Scale bar: 200 μm (left panel), 50 μm (right panel). Upregulation of *c-fos* mRNA in BLA following fear conditioning occurred exclusively in the neurons with upregulation of *egr-1* mRNA. Quantification of *c-fos* and *egr-1* mRNA in BLA of flox mice 30 min after fear conditioning with or without restraint stress revealed that $12.62\% \pm 0.16\%$ or $16.92 \pm 2.70\%$ of *egr-1* positive neurons, respectively, are *c-fos* positive in BLA, $N = 3\text{--}4$ mice in each group. **g** cKO mice with RapGEF2 ablation in BLA showed attenuation in *egr-1* mRNA, but not in *c-fos* mRNA increase in BLA after fear conditioning when acute restraint stress was applied prior to fear conditioning. Upregulation of *c-fos* mRNA in BLA following fear conditioning occurred only in the neurons with upregulation of *egr-1* mRNA. *c-fos* and *egr-1* mRNA signals were quantified by NIH Image J using the mean gray values of integrated density after being converted to gray scale; then normalized to average value from flox mice in the home cage (NFC) to obtain “Relative *c-fos* mRNA level” or “Relative *egr-1* mRNA level”. $N = 3\text{--}4$ for animal number in each group. Two-way ANOVA followed by post hoc Bonferroni t-test, ***** $p < 0.05$, ****** $p < 0.001$

of conditioned fear in mice. Since ERK dependency distinguishes cAMP-dependent from cAMP-independent synaptic potentiation [15], we asked if deletion of a molecular actor involved in neuronal cAMP-dependent activation of ERK, RapGEF2, from hippocampal neurons might impair both cAMP-dependent ERK activation and downstream ERK-dependent immediate early-gene induction, and potentially cognate hippocampus-dependent associative learning (fear conditioning). Our rationale for consideration of RapGEF2 as a novel signaling component crucial for ERK activation

during associative learning derived from observations that RapGEF2 is (i) an obligate cAMP sensor in ERK-dependent Gs-coupled GPCR initiation of neuritogenesis in neuroendocrine cells [38]; (ii) a neuron-specific signaling molecule in adult mammalian brain [31]; (iii) required for dopaminergic cAMP-dependent signaling to ERK underlying cocaine’s psychomotor stimulant effects on behavior [32]; and (iv) required for cAMP-dependent induction of the immediate-early gene *egr1/zif268* [31, 32], implicated in learning and memory mechanisms, along with ERK and cAMP, in hippocampus and other brain areas [5]. The requirement for RapGEF2 for both cAMP-dependent LTP and context-dependent fear conditioning in mice provides a biochemical mechanistic linkage between cAMP, activation of Rap1 which is also implicated in cAMP-dependent LTP at the Schaffer collateral (CA3-CA1) synapse [15, 61], and ERK. This prompted us to further examine immediate-early gene induction associated with fear conditioning in vivo. LTP involves the mobilization of immediate-early genes activated by both the cAMP and calcium pathways. *Fos* up-regulation can be either calcium- or cAMP-dependent, while that of other immediate early genes, such as *egr1*, are cAMP-dependent [5, 32, 62–69]. *Fos* induction initiated either by cAMP or calcium has been attributed variously to a PKA-dependent, Rap1-independent activation of ERK, leading to MSK-1 activation, and phosphorylation/activation of the transcription factor CREB, or to a CREB-dependent mechanism due to CREB phosphorylation directly by PKA [41, 70–72]. *Egr1* induction, on the other hand, is more specifically related to activation of ERK, and associated with stress-related behavioral outcomes involving neuronal plasticity distinct from other IEGs including *fos* [73]. Our finding that *c-Fos* up-regulation after fear conditioning occurs within the same hippocampal neuronal population(s) in which *Egr-1* is also elevated provides solid evidence for the existence of separate (parcellated) signaling pathways for the regulation of these two IEGs.

Fear conditioning is accompanied by ERK activation and *Egr1* induction in amygdala as well as hippocampus, however this apparently occurs independently of cAMP, as suggested by the lack of dependence on RapGEF2 [39] and consistent with previous observations that Rap1-dependent amygdalar involvement in fear conditioning is dependent on unconditioned stimulus intensity [74]. Restraint-augmented fear conditioning, however, does require the recruitment of inputs that employ the cAMP \rightarrow RapGEF2 \rightarrow ERK pathway for induction of *Egr1* and for associative learning. Variations in signal transduction pathways that link first messengers, second messengers, and the immediate early genes that control neuronal plasticity provide the specific biochemical infrastructure for different modes of learning, and especially learning that is strongly associated with emotion. RapGEF2 is not required for the hippocampally-mediated spatial task

tested in the Barnes maze, for example, and this is reminiscent of the effect of Camk2 α -associated Rap1 knockout to impair fear learning while leaving spatial learning intact [74]. Likewise ablation of Ras-GRF1, another guanine nucleotide exchanger involved in ERK activation in neurons, leads to selective impairment in fear conditioning without affecting non-emotional cognitive learning [75].

Establishment of linkage between cAMP-dependent synaptic potentiation, ERK activation and associative learning via a common requirement for RapGEF2 opens several avenues for future research. For example, it is not yet known which isoform(s) of Rap are required for RapGEF2-dependent ERK activation involved in associative learning, in either hippocampus or amygdala. RapGEF2 is linked to activation of Rap1 in the neuroendocrine NS-1 cell line, whereas the cAMP sensor Epac preferentially activates Rap2 [30]. RapGEF2 has been previously implicated in hippocampal signaling as a required component in Plk2-dependent synaptic plasticity in the hippocampus [35], in mir19-dependent regulation of the migration of nascent granule cells in dentate gyrus [34], and in hippocampal synaptic maintenance and cognitive function in a mouse model for Alzheimer Disease [76]. However, the role of Rap isoforms in any RapGEF2-associated synaptic events in the hippocampus remain unclear. Exploration of Rap isoform-dependence of RapGEF2 involvement in cAMP-dependent LTP, and contextual fear conditioning, may shed further light on this, and on RapGEF2 involvement in long-term depression, also implicated in hippocampus-dependent fear conditioning [61, 77, 78].

Finally, RapGEF2 involvement in cAMP-dependent memory function suggests an experimental pathway to identify first messengers associated with memory function via their signaling to ERK via RapGEF2. Frey and Kandel in the first classical experiments describing cAMP-dependent LTP in hippocampus suggested that dopamine, coupled to cAMP elevation through the D1 receptor, might fulfill the role of such a first messenger in the hippocampus [18]. Cyclic AMP \rightarrow RapGEF2 \rightarrow ERK signaling represents a new avenue for dissecting how MAP kinase signaling pathways support complex cognitive processes in hippocampus and amygdala, and exploring how first messengers causing cAMP elevation, physiologically or pharmacologically, contribute to synaptic plasticity in behavioral states in which associative learning occurs.

Methods and materials

Animals

Mice (wild-type or transgenic) on C57BL6J background were housed 2–5 per cage and acclimatized to 12-h

light/12-h dark cycle with food and water ad libitum. Animal care was approved by the NIMH Institutional Animal Care and Use Committee (IACUC) and conducted in accordance with NIH guidelines. The floxed RapGEF2 mouse strain RapGEF2^{fl/fl} and RapGEF2 KO mouse strain Camk2 α -cre^{+/-}::RapGEF2^{fl/fl} (cKO) were generated as described previously [31]. Detailed information about the Camk2 α -cre⁺ strain used to direct Cre expression to excitatory forebrain neurons can be found in the Jackson Labs strain directory under Strain #005359.

Behavioral tests

Animal behavioral tests were conducted in NIMH and NICHD Rodent Behavioral Core Facilities.

Home cage monitoring

Mice were monitored for locomotor activity for two days in individual home cages under normal vivarium conditions using the Photobeam Activity System-Home Cage (PAS-HC) (San Diego Instruments, San Diego, CA, USA).

Elevated zero maze

The elevated zero maze for anxiety was performed by placing the mouse into an open quadrant of a continuous circular 5.5 cm-wide track elevated 65 cm above the floor and divided into alternating walled and open quadrants in a dimly lit room, for 6 min. Video recording from above in the last 5 min was automatically scored for time spent in each quadrant (Top Scan software suite, Clever System Inc.).

Open field

Mice were placed into an open field box (L 17.5 in, H 18.25 in, W 15.25 in) in a dimly lit room (40 lx) to monitor locomotor activity for 1 h. Video recording from above was automatically scored for total travel distance in the box and time spent in the center of the open field using Top Scan software (Clever System).

Rotarod

Rotarod test was performed using an Accurotor rotarod (AccuScan Instruments). Animals were tested concurrently in four separate 11 cm-wide compartments on a rod approximately 3 cm in diameter and elevated 35 cm. The apparatus started at an initial speed of 4 rpm and gradually accelerated at a rate of 0.2 rpm/s. The latency to fall from the rod was recorded with a cut-off time of 2 min. Each animal was assessed over ten trials with 20-min intertrial intervals.

Hot plate

Pain sensitivity of mice was tested using a Hot Plate Analgesia Meter (San Diego Instruments, San Diego, CA, USA). Mice were placed on the hot plate (55 ± 0.1 °C). The mice were constrained to the hot plate by clear acrylic walls (19 cm tall, open top). The latency to respond with either hind paw lick, hind paw flick, or jump was measured, and the mouse was immediately removed from the hot plate and returned to its home cage. The cut-off time was 30 s. Animals were tested individually and were not habituated to the apparatus prior to testing.

Barnes maze

A modified Barnes maze (Patterned Barnes maze, PBM) [79, 80] (Figure S2a) was used to test spatial learning and memory. The PBM consists of a 122 cm diameter circular platform with a height of 91.44 cm. The platform consists of 40 holes; 16 holes in the outer ring, 16 holes in the middle ring and 8 holes in the inner ring. The holes are of diameter 10 cm. A plastic escape tube with a ramp was positioned beneath one of the holes to serve as the escape box. Distal extra-maze visual cues were placed on the walls of the room. The high overhead lighting at 1200 lx was used to create aversive motivation for the subjects. Trials were video recorded and scored by ANY-maze software (ANY-maze, Wood Dale, IL, USA) for measures including latency to find the hidden platform, total distance traveled, and speed. The animals were habituated in the escape box for 60 s one day before training. Training trials included 7 days of training (two trials for each animal daily with 30 min of intertrial interval and 3 min cut-off time for each trial). Animals took a rest for two days and had a probe test on day 10. In the probe trial, the escape box was removed from the target hole and animals were allowed to explore on the platform for 3 min.

Fear conditionin

On day 1 of the experiment, mice were habituated to the test chamber (Med Associates) for 5 min in context A which was used for conditioning. Context A consisted of a square metal chamber, shock grid floor and external chamber light on one side. Context A was cleaned between each trial using 70% ethanol and the testing room was dimly lit. The novel context (Context B) consisted of patterned paper walls, plastic chamber floor and an internal blue light on top of the chamber. Context B was cleaned with household glass cleaner between trials. The testing room was dark for Context B. On day 2, the mouse was exposed to context A for 2.5 min, followed by 1 pairing of a tone (3000 Hz, 85 dB, 30 s) with a foot shock (0.5 mA, 2 s). For some cohorts of mice, 1 h restraint stress

(in DecapiCone, Braintree Scientific) was applied 3 h prior to fear conditioning. Contextual fear memory was tested at 3 or 24 h after fear conditioning by placing the mouse in the training chamber for 3 min. Cued fear memory was tested at 24 h after fear conditioning by exposing the mouse to a tone (3000 Hz, 85 dB, 30 s) following free running for 2.5 min in context B. Freezing was identified as complete immobility (at least 2 s) with the Video Freeze 4 software (Med Associates). The scheme for fear conditioning protocol is presented in Figure S2b.

Western blot

Mice were sacrificed by cervical dislocation and the brain was quickly removed from skull. Mouse brains were rinsed by ice-cold PBS and sectioned with a mouse brain matrix in 500 μ m thick slices. The hippocampal CA1, CA3 and DG were dissected out respectively from slices (from approximately Bregma -1.43 mm to bregma -2.53 mm) in cold PBS under dissecting microscope. Structure boundaries were identified using a mouse brain atlas [81]. Once dissected, samples were immediately frozen in dry ice and later stored at -80 °C. Samples were sonicated on ice with RIPA buffer supplemented with Halt Protease and Phosphatase Inhibitor Cocktail (Thermo Scientific). RIPA-insoluble fractions were removed by centrifugation (3000 rpm for 10 min at 4 °C). Supernatants were retained, and protein concentration was determined by MicroBCA Protein Assay kit (Thermo Scientific) according to the protocol provided by the manufacturer. Western blot was performed as described previously [31]. The rabbit polyclonal anti-GAPDH (D16H11) (Cell Signaling Technology, Cat# 5174; 1:1000), rabbit anti-RapGEF2 (NNLE-2, 1:1000), rabbit polyclonal anti-phospho-p44/42 MAPK (Erk1/2) (Thr202/Tyr204) (Cell Signaling Technology, Cat# 9101; 1:1000) and rabbit polyclonal anti-p44/42 MAPK (Erk1/2) (Cell Signaling Technology, Cat# 9102; 1:1000) were used. Immunoreactive bands were visualized with a SuperSignal West Dura Chemiluminescent Substrate (Thermo Scientific), photographed with a ChemiDoc Imaging system, and quantified with NIH ImageJ.

Histochemistry and microscopy

Immunohistochemistry was conducted as previously described [31] after animal perfusion with 4% paraformaldehyde. Briefly, mouse brains were sectioned by Vibratome at a 40 μ m thickness. Free-floating sections were washed in TBS containing 0.5% Triton X-100 (TBST; 3 washes, 15 min), incubated at room temperature in blocking solution (10% normal goat or donkey serum in TBST; 1 h), and then incubated in primary antibody diluted in blocking solution overnight at 4 °C. The following day, sections were washed in TBST (3 washes, 15 min), incubated in the dark in Alexa

555-conjugated or Alexa 488-conjugated goat anti-rabbit-IgG (1:300; Millipore Sigma) for 2 h following primary antibody incubation. Sections were mounted in Vectashield (Vector Laboratories, Burlingame, CA). The primary antibodies used were rabbit anti-pERK (1:1500, Cell Signaling Technology, Danvers, MA), anti-c-Fos (1:5000, EnCor Biotechnology Inc., Gainesville, FL), anti-Egr-1 (15F7) (1:1000, Cell Signaling Technology, Danvers, MA) and rabbit anti-Rapgef2 (NNLE-2, custom-made by Anaspec [31]). Confocal images were obtained on a Zeiss LSM 510 confocal microscope at the National Institute of Neurological Disorders and Stroke Light Imaging Facility. Immunoreactive (IR) signals of RapGEF2, phospho-ERK, c-Fos and Egr-1 from different brain areas as indicated were quantified by NIH Image J using the mean gray values of integrated density after being converted to gray scale; then normalized to average value from mice in the home cage (NFC) to obtain “Relative IR of phospho-ERK”, “Relative IR of c-Fos” or “Relative IR of Egr-1”.

RNAscope in situ hybridization

In situ hybridization was conducted using the RNAScope Multiplex Fluorescent V2 Kit (Cat# 323,100) (ACD Bio), as directed in the manual. Briefly, fresh-frozen mouse brains were sectioned coronally or sagittally on a cryostat to 12 μm . Sections were mounted on Superfrost Plus slides (Fisher Scientific). Slides were fixed with 4% paraformaldehyde for 20 min at 4 $^{\circ}\text{C}$, then dehydrated in an ethanol gradient. Hydrogen peroxide and protease treatments, probe hybridization and signal development proceeded as described in the manual. Probes were Mm-Fos (Cat No. 316921) and Mm-Egr1-C2 (cat No. 423371-C2). These were developed with Opal 520 and Opal 570 fluorophores (Akoya Biosciences). Confocal images were obtained on a Zeiss LSM 510 confocal microscope at the National Institute of Neurological Disorders and Stroke Light Imaging Facility. C-fos and egr-1 mRNA signals were quantified by NIH Image J using the mean gray values of integrated density after being converted to gray scale; then normalized to average value from mice in the home cage (NFC) to obtain “Relative c-fos mRNA level” or “Relative egr-1 mRNA level”.

snRNA-seq

Thirty minutes after fear conditioning, mice were decapitated and whole brain was extracted quickly and put into the cold PBS for a brief rinse. Coronal section containing the dorsal hippocampus were prepared using a metal mouse brain matrix and CA1 subregions (2 tissue blocks/animal) were dissected out and snap frozen in the dry ice and kept at -80°C freezer until further assay. CA1 tissue from three animals per group (home cage group or fear conditioning

group) were pooled together and processed to prepare the single nuclei samples. Briefly, the tissue was minced in pre-chilled detergent lysis buffer (low sucrose buffer with 0.1% Triton X-100) using a Dounce homogenizer, followed by passing the crude nuclei prep through a strainer (pore size 40 μm) to remove cellular aggregates. After centrifugation, the pellet was resuspended in the low sucrose buffer (11% Sucrose, 10 μM pH 8.0 HEPES, 5 μM CaCl_2 , 3 μM MgAc_2 , 0.1 μM EDTA and 1 μM DTT) and homogenized using an electronic homogenizer to dissociate the nuclei from the protein. Then, centrifuge was performed by putting a layer of density sucrose buffer (34% sucrose, 10 μM pH 8.0 HEPES, 3 μM MgAc_2 and 1 μM DTT) underneath the low sucrose buffer homogenate to purify the nuclei prep. Ten microliter nuclei were mixed with trypan blue to manually determine the proportion of nuclei and nuclei concentrations using a hemocytometer. Final nuclei concentration was adjusted to ~ 1000 nuclei/ μL and a total of around 5000–6000 nuclei was used for subsequent library generation. cDNA libraries were constructed following manufacture’s instruction (Chromium Next GEM Single Cell 3’ Reagents Kits V3.1 User Guide, 10 \times Genomics). Briefly, nuclei were mixed with reverse transcription mix and loaded into the chip. The mRNAs of single nuclei were captured by barcoded beads using a Chromium controller. Reverse transcribed cDNAs were then PCR amplified, fragmented, and ligated with adaptors followed by sample index PCR. cDNA libraries were sequenced on an Illumina Nextseq 500/500 High output kit v2.5 (150 Cycles) and the alignment of raw sequencing reads to the mouse genome was conducted using the 10 \times Genomics Cell Ranger pipeline (version 7.0.1) to obtain cell by gene matrices for subsequent downstream analysis. Samples from three cohorts of experiments were imported and integrated with the Seurat package, analyzed using Partek flow software following manufacture’s manual.

Hippocampal slice preparation, electrophysiology, data acquisition and analysis

Hippocampal slice preparation

The first step of acute hippocampal slice preparation was cardiac perfusion with ice-cold cutting solution which contained (in mM): 215 sucrose, 2.5 KCl, 20 glucose, 26 NaHCO_3 , 1.6 NaH_2PO_4 , 0.5 CaCl_2 , 4 MgCl_2 , 4 MgSO_4 . Next, the hippocampi were isolated from the brain, and placed in an agar template to allow transverse sectioning at 400 μm thickness with a VT1000S vibratome (Leica). The resulting slices were immediately transferred to a solution composed of 50% Cutting solution and 50% recording solution (50–50 solution) for 30 min. The recording solution contained (in mM): 124 NaCl, 2.5 KCl, 26 NaHCO_3 , 1 NaH_2PO_4 , 2 CaCl_2 , 1.3 MgSO_4 and 10 glucose. All solutions

were equilibrated with 95% O₂ and 5% CO₂. Next, the 50–50 solution was replaced by 100% recording solution and incubated for an additional hour at room temperature, after which the slices were considered as ready for experiments.

Slice electrophysiology

Hippocampal slices were chosen for experiments after visualization using infrared differential interference contrast (IR/DIC) and ensured to be intact. Hippocampal slices were continuously perfused, in a submerged chamber, with fresh aCSF at a rate of 2 ml per min at 32 °C. Electrical stimulations were induced by a monopolar electrode which delivered square-wave current pulses of 0.1 ms duration. The currents were generated by a stimulus isolator (Isoflex, AMPI) connected to a borosilicate glass pipette pulled by a pipette puller (Narishige) to a tip size of ~5 μm. fEPSPs were recorded using a patch pipette filled with 0.5 M NaCl (2–3 MΩ) connected to an EPC10 amplifier (HEKA). For measurements in the hippocampal medial perforant pathway (MPP), the stimulating electrode was placed in the middle molecular layer of the DG near the vertex of the DG. The recording electrode was also placed at the middle molecular layer of the DG, but more laterally towards the tip of the upper blade. For measurements in the hippocampal Schaffer Collateral (SC) pathway, the stimulating was placed in the *stratum radiatum* of the CA1 subregion, near its border with the CA2 subregion. The recording electrode was also placed in the *stratum radiatum* of the CA1 subregion, but more downstream to the stimulating electrode, towards the subiculum. Stimulation intensity and electrode placement were calibrated to yield clean fEPSPs of an amplitude of 0.5–0.8 mV. fEPSPs were elicited by delivering paired pulses of 25 Hz once every 20 s. Before each experiment, a stable baseline of at least 20 min was ensured.

Data acquisition and statistical analysis

Electrophysiology data was acquired using the PatchMaster software (Heka). The recorded files were then exported into CSV files using Igor Pro 6.22A (Wavemetrics), and further analyzed using custom-made MATLAB scripts. Specifically, the traces were first smoothed using the Savitzky-Golay method, in order to remove high-frequency noise. Next, unless stated otherwise, each fEPSPs was calculated as the slope between 20 and 80 percentiles of the EPSP trace, manually selected from the base to the peak of the EPSP component. The calculated of the responses were then normalized by transforming the values into percentages of the baseline response $\left(\frac{fEPSP_{absolute\ slope}}{mean\ of\ baseline\ fEPSP\ slopes} \times 100 \right)$. The facilitation was calculated using the paired-pulse ratio parameter

which measures the ratio between the responses to two stimuli given in short order (ISI = 40 ms, PPR = $\frac{fEPSP\ of\ the\ second\ stimulus}{fEPSP\ of\ the\ first\ stimulus}$).

Statistical analyses were done using Graphpad Prism 8 software. Results are reported as the mean ± SEM. Statistical significance was set to $p < 0.05$ (marked by *; $p < 0.01$ and $p < 0.001$ were signified using ** and ***, respectively). The statistical test used was repeated measures two-way ANOVA for most cases. All MATLAB scripts are available upon request.

Reagents

Forskolin (Cat #1099), U0126 (Cat #1144) and bicuculline (Cat #0130) were purchased from Tocris Bioscience (Bristol, UK), and were used at concentrations of 25, 20 and 10 μM, respectively. U0126 incubation was begun 20 min before addition of forskolin and continued for 40 min. All working solutions contained ≤ 0.1% DMSO.

Experimental design and statistical analysis

Mice of both sexes were used in all studies. The sample size (n) per group is indicated in the figure legends for each experiment. Statistical analyses were conducted using Sigma Plot 14.0 (Systat Software). Student's t-tests and factorial model analysis of variances (ANOVA) were employed where appropriate. Post hoc analyses were performed using the *Bonferroni* Test. Data were reported using histograms and scatter plots to represent mean ± s.e.m and individual data in each group. Differences were considered to be significant when $p < 0.05$.

Supplementary Information The online version contains supplementary material available at <https://doi.org/10.1007/s00018-023-04999-y>.

Author contributions All authors contributed to the study conception and design. Material preparation, data collection and analysis were performed by SZJ, MS, H-YZ, WB and AE. All authors wrote and commented on the previous versions of manuscript, and read and approved the final manuscript.

Funding This work was supported by NIMH-IRP Project MH002386 to L.E.E., supplemental NIMH-IRP funding to the Dendritic Dynamics Hub (L.E.E., and H.A.T.), grants from Israel Science Foundation (ISF grants 953/16 and 2141/20) and the DFG (NA: 207/10-1), the Taube/Koret Global Collaboration in Neurodegenerative Diseases and the BrightFocus grant (A2022029S), NIH grant 1R21AG074846-01A1, and the Michael J. Fox Foundation (MJFF-022407) to UA, and training grant, a Brain and Behavior Research Foundation NARSAD Young Investigator Award and supplemental DDH funding to M.S.

Data availability The datasets generated and analysed during the current study are available from the corresponding author on reasonable request.

Declarations

Conflict of interest The authors declare no competing interests.

Ethical approval Animal studies was approved by the NIMH Institutional Animal Care and Use Committee (IACUC) and conducted in accordance with NIH guidelines.

Consent to participate No human subjects were involved.

Consent to publish No human subjects were involved.

References

- Sudhof TC, Malenka RC (2008) Understanding synapses: past, present, and future. *Neuron* 60(3):469–476
- Kandel ER (2001) The molecular biology of memory storage: a dialogue between genes and synapses. *Science* 294:1030–1038
- Alberini CM, Kandel ER (2015) The regulation of transcription in memory consolidation. *Cold Spring Harb Perspect Biol* 7(1):a021741
- Malenka RC, Bear MF (2004) LTP and LTD: an embarrassment of riches. *Neuron* 44(1):5–21
- Bozon B, Kelly A, Josselyn SA, Silva AJ, Davis S, Laroche S (2003) MAPK, CREB and zif268 are all required for the consolidation of recognition memory. *Phil Trans R Soc Lond B Biol Sci* 358(1432):805–814
- Bailey CP, Nicholls RE, Zhang XL, Zhou ZY, Muller W, Kandel ER et al (2008) Galpha(i2) inhibition of adenylyl cyclase regulates presynaptic activity and unmasks cGMP-dependent long-term depression at Schaffer collateral-CA1 hippocampal synapses. *Learn Mem* 15(4):261–270
- Greengard P (2001) The neurobiology of slow synaptic transmission. *Science* 294:1024–1030
- Ferguson GD, Storm DR (2004) Why calcium-stimulated adenylyl cyclases? *Physiology* 19:271–276
- Schwartz JH (1993) Cognitive kinases. *Proc Natl Acad Sci U S A* 90(18):8310–8313
- Shaywitz AJ, Greenberg ME (1999) CREB: A stimulus-induced transcription factor activated by a diverse array of extracellular signals. *Annu Rev Biochem* 68:821–861
- Rosenblum K, Futter M, Voss K, Erent M, Skehel PA, French P et al (2002) The role of extracellular regulated kinases I/II in late-phase long-term potentiation. *J Neurosci* 22(13):5432–5441
- Athos J, Impey S, Pineda VV, Chen X, Storm DR (2002) Hippocampal CRE-mediated gene expression is required for contextual memory formation. *Nat Neurosci* 5(11):1119–1120
- Impey S, Obrietan K, Wong ST, Poser S, Yano S, Wayman G et al (1998) Cross talk between ERK and PKA is required for Ca²⁺ stimulation of CREB-dependent transcription and ERK nuclear translocation. *Neuron* 21(4):869–883
- Impey S, Obrietan K, Storm DR (1999) Making new connections: role of ERK/MAP kinase signaling in neuronal plasticity. *Neuron* 23(1):11–14
- Morozov A, Muzzio IA, Bourchouladze R, Van-Strien N, Lapidus K, Yin D et al (2003) Rap1 couples cAMP signaling to a distinct pool of p42/44MAPK regulating excitability, synaptic plasticity, learning, and memory. *Neuron* 39(2):309–325
- Eckel-Mahan KL, Phan T, Han S, Wang H, Chan GC, Scheiner ZS et al (2008) Circadian oscillation of hippocampal MAPK activity and cAMP: implications for memory persistence. *Nat Neurosci* 11(9):1074–1082
- Sacktor TC, Osten P, Valsamis H, Jiang X, Naik MU, Sublette E (1993) Persistent activation of the z isoform of protein kinase C in the maintenance of long-term potentiation. *Proc Natl Acad Sci USA* 90:8342–46
- Frey U, Huang YY, Kandel ER (1993) Effects of cAMP simulate a late stage of LTP in hippocampal CA1 neurons. *Science* 260(5114):1661–1664
- Lledo P-M, Hjelmstad GO, Mukherji S, Soderling TR, Malenka RC, Nicoll RA (1995) Calcium/calmodulin-dependent kinase II and long-term potentiation enhance synaptic transmission by the same mechanism. *Proc Natl Acad Sci USA* 92:11175–11179
- Abel T, Nguyen PV, Barad M, Deuel TA, Kandel ER, Bourchouladze R (1997) Genetic demonstration of a role for PKA in the late phase of LTP and in hippocampus-based long-term memory. *Cell* 88(5):615–626
- Atkins CM, Selcher JC, Petraitis JJ, Trzaskos JM, Sweatt JD (1998) The MAPK cascade is required for mammalian associative learning. *Nat Neurosci* 1(7):602–609
- Collingridge GL, Bliss TVP (1995) Memories of NMDA receptors and LTP. *TINS* 18:54–56
- Abraham WC, Jones OD, Glanzman DL (2019) Is plasticity of synapses the mechanism of long-term memory storage? *NPJ Sci Learn* 4:9
- Adams JP, Sweatt JD (2002) Molecular psychology: roles for the ERK MAP kinase cascade in memory. *Annu Rev Pharmacol Toxicol* 42:135–163
- de Rooij J, Zwartkruis FJT, Verheijen MHG, Cool RH, Jijman SMB, Wittinghofer A et al (1998) Epac is a Rap1 guanine-nucleotide-exchange factor directly activated by cyclic AMP. *Nature* 396:474–477
- Kawasaki H, Springett GM, Mochizuki N, Toki S, Nakaya M, Matsuda M et al (1998) A family of cAMP-binding proteins that directly activate Rap1. *Science* 282:2275–2279
- Gloerich M, Bos JL (2010) Epac: defining a new mechanism for cAMP action. *Annu Rev Pharmacol Toxicol* 50:355–375
- Enserink JM, Christensen AE, de Rooij J, van Triest M, Schwede F, Genieser HG et al (2002) A novel Epac-specific cAMP analogue demonstrates independent regulation of Rap1 and ERK. *Nat Cell Biol* 4(11):901–906
- Emery AC, Eiden LE (2012) Signaling through the neuropeptide GPCR PAC1 induces neuritogenesis via a single linear cAMP- and ERK-dependent pathway using a novel cAMP sensor. *FASEB J* 26:3199–3211
- Emery AC, Xu W, Eiden MV, Eiden LE (2017) Guanine nucleotide exchange factor Epac2-dependent activation of the GTP-binding protein Rap2A mediates cAMP-dependent growth arrest in neuroendocrine cells. *J Biol Chem* 292(29):12220–12231
- Jiang SZ, Xu W, Emery AC, Gerfen CR, Eiden MV, Eiden LE (2017) NCS-Rapgef2, the protein product of the neuronal Rapgef2 gene, is a specific activator of D1 dopamine receptor-dependent ERK phosphorylation in mouse brain. *eNeuro*. <https://doi.org/10.1523/ENEURO.0248-17.2017>
- Jiang SZ, Sweat S, Dahlke S, Loane K, Drossel G, Xu W et al (2021) Cocaine-dependent acquisition of locomotor sensitization and conditioned place preference requires D1 dopaminergic signaling through a cyclic AMP, NCS-Rapgef2, ERK and Egr-1/Zif268 pathway. *J Neurosci* 41:711–725
- Girault JA, Valjent E, Caboche J, Herve D (2007) ERK2: a logical AND gate critical for drug-induced plasticity? *Curr Opin Pharmacol* 7(1):77–85
- Han J, Kim HJ, Schafer ST, Paquola A, Clemenson GD, Toda T et al (2016) Functional implications of miR-19 in the migration of newborn neurons in the adult brain. *Neuron* 91:79–89
- Lee KJ, Lee Y, Rozeboom A, Lee JY, Udagawa N, Hoe HS et al (2011) Requirement for Plk2 in orchestrated ras and rap

- signaling, homeostatic structural plasticity, and memory. *Neuron* 69(5):957–973
36. Phillips RG, LeDoux JE (1992) Differential contribution of amygdala and hippocampus to cued and contextual fear conditioning. *Behav Neurosci* 106(2):274–285
 37. LeDoux JE (2000) Emotion circuits in the brain. *Annu Rev Neurosci* 23:155–184
 38. Emery A, Eiden MV, Mustafa T, Eiden LE (2013) GPCR-Gs signaling to ERK is controlled by the cAMP-sensing guanine nucleotide exchange factor NCS/Rapgef2 in neuronal and endocrine cells. *Sci Signal*. 6:ra51
 39. Emery AC, Eiden MV, Eiden LE (2014) Separate cyclic AMP sensors for neurogenesis, growth arrest, and survival of neuroendocrine cells. *J Biol Chem* 289(14):10126–10139
 40. Xu W, Dahlke SP, Emery AC, Sung M, Chepurny OG, Holz GG, Eiden LE (2021) Cyclic AMP-dependent activation of ERK via GLP-1 receptor signalling requires the neuroendocrine cell-specific guanine nucleotide exchanger NCS-RapGEF2. *J Neuroendocrinol* 33(7):e12974. <https://doi.org/10.1111/jne.12974>
 41. Sindreu CB, Scheiner ZS, Storm DR (2007) Ca²⁺-stimulated adenylyl cyclases regulate ERK-dependent activation of MSK1 during fear conditioning. *Neuron* 53(1):79–89
 42. Harada T, Morooka T, Ogawa S, Nishida E (2001) ERK induces p35, a neuron-specific activator of Cdk5, through induction of Egr1. *Nat Cell Biol* 3(5):453–459
 43. Adams KW, Kletsov S, Lamm RJ, Elman JS, Mullenbrock S, Cooper GM (2017) Role for Egr1 in the transcriptional program associated with neuronal differentiation of PC12 cells. *PLoS ONE* 12(1):e0170076
 44. Han JH, Kushner SA, Yiu AP, Cole CJ, Matynia A, Brown RA et al (2007) Neuronal competition and selection during memory formation. *Science* 316(5823):457–460
 45. Gallo FT, Kathe C, Morici JF, Medina JH, Weisstaub NV (2018) Immediate early genes, memory and psychiatric disorders: focus on c-Fos, Egr1 and Arc. *Front Behav Neurosci* 12:79
 46. Liu X, Ramirez S, Pang PT, Puryear CB, Govindarajan A, Deisseroth K et al (2012) Optogenetic stimulation of a hippocampal engram activates fear memory recall. *Nature* 484(7394):381–385
 47. Ramirez S, Liu X, Lin PA, Suh J, Pignatelli M, Redondo RL et al (2013) Creating a false memory in the hippocampus. *Science* 341(6144):387–391
 48. Liu X, Ramirez S, Tonegawa S (2014) Inception of a false memory by optogenetic manipulation of a hippocampal memory engram. *Philos Trans R Soc Lond B Biol Sci* 369(1633):20130142
 49. Roozendaal B, McEwen BS, Chattarji S (2009) Stress, memory and the amygdala. *Nat Rev Neurosci* 10(6):423–433
 50. Schafe GE, Atkins CM, Swank MW, Bauer EP, Sweatt JD, LeDoux JE (2000) Activation of ERK/MAP kinase in the amygdala is required for memory consolidation of pavlovian fear conditioning. *J Neurosci* 20(21):8177–8187
 51. Schafe GE, Swank MW, Rodrigues SM, Debiec J, Doyere V (2008) Phosphorylation of ERK/MAP kinase is required for long-term potentiation in anatomically restricted regions of the lateral amygdala in vivo. *Learn Mem* 15(2):55–62
 52. Briand LA, Blendy JA (2013) Not all stress is equal: CREB is not necessary for restraint stress reinstatement of cocaine-conditioned reward. *Behav Brain Res* 246:63–68
 53. Selcher JC, Atkins CM, Trzaskos JM, Paylor R, Sweatt JD (1999) A necessity for MAP kinase activation in mammalian spatial learning. *Learn Mem* 6(5):478–490
 54. Sweatt JD (2004) Mitogen-activated protein kinases in synaptic plasticity and memory. *Curr Opin Neurobiol* 14(3):311–317
 55. Shalin SC, Egli R, Birnbaum SG, Roth TL, Levenson JM, Sweatt JD (2006) Signal transduction mechanisms in memory disorders. *Prog Brain Res* 157:25–41
 56. Lynch MA (2004) Long-term potentiation and memory. *Physiol Rev* 84(1):87–136
 57. Bromer C, Bartol TM, Bowden JB, Hubbard DD, Hanka DC, Gonzalez PV et al (2018) Long-term potentiation expands information content of hippocampal dentate gyrus synapses. *Proc Natl Acad Sci U S A* 115(10):E2410–E2418
 58. Silva AJ, Kogan JH, Frankland PW, Kida S (1998) CREB and memory. *Annu Rev Neurosci* 21:127–148
 59. Winder DG, Martin KC, Muzzio IA, Rohrer D, Chruscinski A, Kobilka B et al (1999) ERK plays a regulatory role in induction of LTP by theta frequency stimulation and its modulation by beta-adrenergic receptors. *Neuron* 24(3):715–726
 60. Bliss TV, Collingridge GL, Morris RGM, Reymann KG (2018) Long-term potentiation in the hippocampus: discovery, mechanisms and function. *Neuroforum* 24:A103–A120
 61. Zhang L, Zhang P, Wang G, Zhang H, Zhang Y, Yu Y et al (2018) Ras and Rap signal bidirectional synaptic plasticity via distinct subcellular microdomains. *Neuron*. 98(4):783–800 e4
 62. Sheng M, Greenberg ME (1990) The regulation and function of c-fos and other immediate early genes in the nervous system. *Neuron* 4:477–485
 63. Sheng M, McFadden G, Greenberg ME (1990) Membrane depolarization and calcium induce c-fos transcription via phosphorylation of transcription factor CREB. *Neuron* 4:447–485
 64. Greenberg ME, Thompson MA, Sheng M (1992) Calcium regulation of immediate early gene transcription. *J Physiol* 86:99–108
 65. Ginty DD, Bading H, Greenberg ME (1992) Trans-synaptic regulation of gene expression. *Curr Opin Neurobiol* 2:312–316
 66. Tai TC, Morita K, Wong DL (2001) Role of Egr-1 in cAMP-dependent protein kinase regulation of the phenylethanolamine N-methyltransferase gene. *J Neurochem* 76(6):1851–1859
 67. Bozon B, Davis S, Laroche S (2002) Regulated transcription of the immediate-early gene Zif268: mechanisms and gene dosage-dependent function in synaptic plasticity and memory formation. *Hippocampus* 12(5):570–577
 68. Ravni A, Vaudry D, Gerdin MJ, Eiden MV, Falluel-Morel A, Gonzalez B et al (2008) A cAMP-dependent, PKA-independent signaling pathway mediating neurogenesis through Egr1 in PC12 cells. *Mol Pharmacol* 73:1688–1708
 69. Gangarossa G, Di Benedetto M, O’Sullivan GJ, Dunleavy M, Alcacer C, Bonito-Oliva A et al (2011) Convulsant doses of a dopamine D1 receptor agonist result in Erk-dependent increases in Zif268 and Arc/Arg3.1 expression in mouse dentate gyrus. *PLoS One*. 6(5):e19415
 70. Wong ST, Athos J, Figueroa XA, Pineda VV, Schaefer ML, Chavkin CC et al (1999) Calcium-stimulated adenylyl cyclase activity is critical for hippocampus-dependent long-term memory and late-phase LTP. *Neuron* 23:787–798
 71. Poser S, Storm DR (2001) Role of Ca²⁺-stimulated adenylyl cyclases in LTP and memory formation. *Int J Dev Neurosci* 19(4):387–394
 72. Xia Z, Storm DR (2012) Role of signal transduction crosstalk between adenylyl cyclase and MAP kinase in hippocampus-dependent memory. *Learn Mem* 19(9):369–374
 73. Marballi KK, Gallitano AL (2018) Immediate early genes anchor a biological pathway of proteins required for memory formation, long-term depression and risk for schizophrenia. *Front Behav Neurosci* 12:23
 74. Pan BX, Vautier F, Ito W, Bolshakov VY, Morozov A (2008) Enhanced cortico-amygdala efficacy and suppressed fear in absence of Rap1. *J Neurosci* 28(9):2089–2098
 75. d’Isa R, Clapcote SJ, Voikar V, Wolfer DP, Giese KP, Brambilla R et al (2011) Mice lacking Ras-GRF1 show contextual fear conditioning but not spatial memory impairments: convergent evidence from two independently generated mouse mutant lines. *Front Behav Neurosci* 5:78

76. Jang YN, Jang H, Kim GH, Noh JE, Chang KA, Lee KJ (2021) RAPGEF2 mediates oligomeric Abeta-induced synaptic loss and cognitive dysfunction in the 3xTg-AD mouse model of Alzheimer's disease. *Neuropathol Appl Neurobiol* 47(5):625–639
77. Ryu J, Futai K, Feliu M, Weinberg R, Sheng M (2008) Constitutively active Rap2 transgenic mice display fewer dendritic spines, reduced extracellular signal-regulated kinase signaling, enhanced long-term depression, and impaired spatial learning and fear extinction. *J Neurosci* 28(33):8178–8188
78. Stornetta RL, Zhu JJ (2011) Ras and Rap signaling in synaptic plasticity and mental disorders. *The Neuroscientist* 17(1):54–78
79. Barnes CA (1979) Memory deficits associated with senescence: a neurophysiological and behavioral study in the rat. *J Comp Physiol Psychol* 93(1):74–104
80. Faizi M, Bader PL, Saw N, Nguyen TV, Beraki S, Wyss-Coray T et al (2012) Thy1-hAPP(Lond/Swe+) mouse model of Alzheimer's disease displays broad behavioral deficits in sensorimotor, cognitive and social function. *Brain Behav* 2(2):142–154
81. Franklin KBJ, Paxinos G (2019) The mouse brain in stereotaxic coordinates. Academic Press, New York

Publisher's Note Springer Nature remains neutral with regard to jurisdictional claims in published maps and institutional affiliations.